# Spectroscopic and Magnetic Properties of α-$Li_3Fe_2(PO_4)_3$: A Two-Sublattice Ferrimagnet

A. Goñi,[†] L. Lezama,[†] N. O. Moreno,[‡] L. Fournès,[§] R. Olazcuaga,[§] G. E. Barberis,[‡] and T. Rojo*,[†]

*Dpto. Química Inorgánica, F. Ciencias, UPV/EHU, Apdo. 644, 48080, Bilbao, Spain; Instituto de Física Gleb Wataghin, UNICAMP, 13087−970 Campinas (SP), Brazil; and Institut de Chimie de la Matière Condensée de Bordeaux, Château Brivazac, Avenue du Dr. A. Schweitzer, 33608 Pessac-Cedex, France*

*Received May 21, 1999. Revised Manuscript Received October 11, 1999*

Spectroscopic and magnetic studies on α-$Li_3Fe_2(PO_4)_3$ show an interesting behavior below the transition temperature (29 K). The compound orders antiferromagnetically, presenting a weak ferromagnetic moment, which diminishes with temperature. In the same region of temperatures, the Mössbauer spectra split in two sextets with slightly different hyperfine fields, and the ESR spectrum reduces its intensity and broadens. These results are interpreted as the competition between two sublattices of Fe(III) ions, corresponding to the presence of two independent Fe(III) crystallographic sites in the structure. The magnetic interaction in each sublattice is ferromagnetic, being coupled antiferromagnetically between them. The observed weak ferromagnetic component is the result of the ferrimagnetic character in the coupling between two Fe(III) sublattices.

## Introduction

The study of phosphates with fast ion transport properties has been intensive since the discovery of the "Nasicon" system.[1] The $Li_3M_2(PO_4)_3$ (M = Cr, Sc, In, Fe, and so on) compounds have been considered as very interesting materials, due to their potential application as lithium solid-state electrolytes.[2,3]

The relationship between the structural and spectroscopic properties and the ion transport properties has been extensively investigated on the series of the $Li_3M_2(PO_4)_3$ phosphates.[4−8] These compounds are considered as solid electrolytes, although they do not show high ionic conductivity at room temperature ($10^{-5}$ S cm$^{-1}$ for ceramic samples). However, structural phase transitions occurring in the 470−820 K temperature range lead to an increase of disorder in the lithium ions subsystem in the crystal net, inducing the ionic mobility in the samples. In this way, $Li_3Fe_2(PO_4)_3$ exhibits high ionic conductivity ($10^{-2}$ S cm$^{-1}$) at 573 K and rather low ionic activation energy values (in the 0.3−0.6 eV range), being considered as belonging to the group of the superionic conductors.[9] Moreover, the presence of $Fe^{3+}$ ions in the crystal net could induce the existence of interesting magnetic properties in this material. As far as we are aware, magnetic studies on this phase have not been carried out.

The crystal structure of α-$Li_3Fe_2(PO_4)_3$ at room temperature consists of a three-dimensional framework of slightly distorted $FeO_6$ octahedra and $PO_4$ tetrahedra sharing by oxygen vertexes.[10] Each $FeO_6$ octahedron is surrounded by six $PO_4$ polyhedra. Each $PO_4$ tetrahedron is linked to four $FeO_6$ polyhedra, forming a three-dimensional mixed heterogeneous framework, which can be described by the general formula $\{Fe_2[PO_4]_3\}^{3-}$. The lithium ions occupy three different crystallographic positions in the structure: one of them in the center of a regular tetrahedron with oxygen atoms and the other two inside distorted trigonal bipyramids.

There are two independent crystallographic positions for the Fe(III) ions in the structure of α-$Li_3Fe_2(PO_4)_3$, and consequently, two slightly different $FeO_6$ octahedra. The two independent octahedra are pseudosymmetric by the $[^1/_2 + x, ^1/_2 - y, z]$ pseudosymmetry element, but they are not exactly mirror images by the *ac* crystallographic plane. So, the two independent $FeO_6$ octahedra exhibit small differences in the bond distances and angles. Similar distribution for the Fe(III) ions was found in the structures of the $Fe_2(SO_4)_3$[11,12] and $Fe_2$-

* E-mail: qiproapt@lg.ehu.es. Fax: 34-94-4648500. Phone: 34-94-6012458.
[†] UPV/EHU.
[‡] UNICAMP.
[§] Institut de Chimie de la Matière Condensée de Bordeaux.

(1) Hong, H. Y. P. *Mater. Res. Bull.* **1976**, *11*, 173.
(2) Julien, C.; Nazri, G. A. *Solid State Batteries: Materials Design and Optimization*; Kluwer Academic Publishers: Boston, 1994.
(3) Masquelier, C.; Padhi, A. K.; Nanjundaswamy, K. S.; Goodenough, J. B. *J. Solid State Chem.* **1998**, *135*, 228.
(4) d'Yvoire, F.; Pintard-Scrépel, M.; Bretey, E.; de la Rochère, M. *Solid State Ionics* **1983**, *9−10*, 851.
(5) Lyubutin, I. S.; Melnikov, O. K.; Sigaryov, S. E.; Terziev, V. G. *Solid State Ionics* **1988**, *31*, 197.
(6) Kravchenko, V. V.; Sigaryov, S. E. *Solid State Commun.* **1992**, *83* (2), 149.
(7) Winand, J. M.; Rulmont, A.; Tarte, P. *J. Solid State Chem.* **1990**, *87*, 83.
(8) Padhi, A. K.; Nanjundaswamy, K. S.; Masquelier, C.; Okada, S.; Goodenough, J. B. *J. Electrochem. Soc.* **1997**, *144* (5), 1609.
(9) Sigaryov, S. E.; Terziev, V. G. *Phys. Rev. B* **1993**, *48* (22), 16252.
(10) Bykov, A. B.; Chirkin, A. P.; Demyanets, L. N.; Doronin, S. N.; Genika, E. A.; Ivanov-Shits, A. K.; Kondratyuk, I. P.; Maksimov, B. A.; Mel'nikov, O. K.; Mudaryan, L. N.; Simonov, V. I.; Timofeeva, V. A. *Solid State Ionics* **1990**, *38*, 31.
(11) Moore, P. B.; Araki, T. *Neues Jahrb. Mineral. Abh.* **1974**, *121*, 208.

10.1021/cm991069c CCC: $19.00 
Published on Web 12/11/1999

$(MoO_4)_3$[13] related compounds. The magnetic studies on these phases[14,15] revealed interesting type-L[16] ferrimagnetic behavior, as a result of the magnetic coupling between the two different iron sublattices.

In this paper, we describe the study of the magnetic properties and Mössbauer spectroscopy on α-$Li_3Fe_2(PO_4)_3$ at low temperatures.

## Experimental Section

**Synthesis and Initial Characterization.** $Li_3Fe_2(PO_4)_3$ was prepared by the ceramic method. Stoichiometric amounts of $Fe(NO_3)_3 \cdot 9H_2O$, $H_2NH_4PO_4$ and $LiOH \cdot H_2O$ reagents were homogenized in an agate mortar. The resulting mixture was submitted to three consecutive thermal treatments at 573, 773, and 1073 K, with the corresponding homogenization of the sample following each treatment. The metal ions and phosphorus contents were confirmed by inductively coupled plasma atomic emission spectroscopy (ICP-AES) analysis. The results of the analysis were Li, 5.0(1); Fe 27.0(1); P, 21.8(3)%. $Li_3Fe_2(PO_4)_3$ requires Li, 4.99; Fe, 26.76; P, 22.26%.

The X-ray diffraction (XRD) pattern of the sample was carried out in 10−70° 2$\theta$ range. This pattern was indexed with the cell parameters $a = 8.565(3)$, $b = 12.012(2)$, and $c = 8.617(2)$ Å and $\gamma = 90.54(3)°$, using the space group $P2_1/n$. The very good agreement between the experimental and theoretical diffraction data obtained by Bykov et al. [10] ($a = 8.562(2)$, $b = 12.005(3)$, and $c = 8.612(2)$ Å and $\gamma = 90.51(2)°$) confirmed the identification of the product as α-$Li_3Fe_2(PO_4)_3$. No impurities were detected in the sample by this technique.

**Physical Measurements.** Analytical measurements were carried out by ICP-AES analysis, with an ARL 3410+ ICP with Minitorch equipment. X-ray diffraction pattern was obtained with a Philips 1470 diffractometer, using Cu K$\alpha_1$ radiation. The ESR spectra were recorded on powdered sample at X-band frequency, with a Bruker ESP300 spectrometer equipped with standard Oxford low-temperature devices and calibrated by an NMR probe for the magnetic field. The frequency was measured with a HP 5352B microwave frequency counter. The magnetic measurements in the 1.8−300 K temperature range (maximum applied field 7 T) were obtained with a Quantum Design MPMS-7 SQUID magnetometer and AC susceptometer. The Mössbauer spectra were measured from 4.2 to 293 K with a classical device described elsewhere.[17] The samples contained less than 10 mg/cm$^2$ of natural iron, a concentration for which the line broadening due to the thickness effects is not noticeable. All isomer shifts reported in this work refer to the natural α-Fe at 293 K.

## Results and Discussion

**EPR Spectroscopy.** The X-band EPR spectra of α-$Li_3Fe_2(PO_4)_3$ were measured in the 4.2−300 K temperature range, and they are shown in Figure 1a. The spectrum at room temperature shows an isotropic signal with a $g$ value of 2.00. This result is in good agreement with the presence of a high-spin Fe(III) ($^6S_{5/2}$) ion in octahedral coordination, with small distortions from the regular shape. The good fitting of Lorentzian derivative to the spectrum indicated that in this system the magnetic exchange interactions predominate over the dipolar ones.

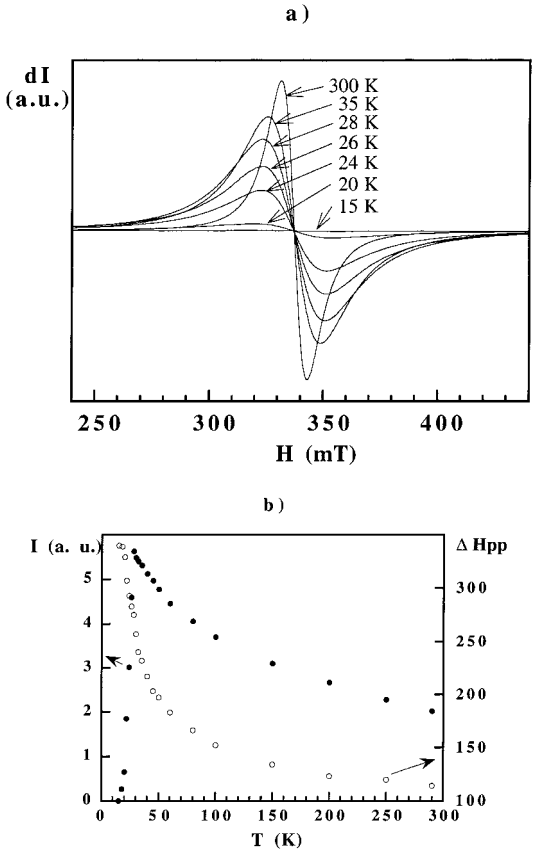


**Figure 1.** (a) Experimental X-band EPR spectra of α-$Li_3Fe_2(PO_4)_3$ at different temperatures, (b) thermal evolution of line width, $\Delta H_{pp}$, and intensity, $I$, of the ESR signal.

No significant variation of the $g$ value was observed in the ESR spectra obtained in all temperature ranges. The line broadens as the temperature decreases, at the same time that the intensity grows (see Figure 1a). The signal begins to reduce abruptly its intensity at about 28 K and finally disappears near 15 K. The thermal evolution of the peak-to-peak line width, $\Delta H_{pp}$, together with the variation of the intensity of the ESR signal has been represented in Figure 1b. The line-width values present a slight increase from 300 to 100 K. Below this temperature, the slope of the $\Delta H_{pp}$ versus $T$ curve becomes substantially higher. With decreasing temperature, the intensity values show an increasing tendency, reaching a maximum at 28 K. At lower temperatures, the intensity value falls toward zero. This behavior allows one to conclude that the magnetic arrangement has been established around 28 K, in α-$Li_3Fe_2(PO_4)_3$. In the magnetic ordered state, the magnetic moments of iron ions are completely coupled, and as a result, the resonance signal becomes undetectable.

**Magnetic Measurements.** The thermal evolution of the molar magnetization, $M$, and $MT$ for α-$Li_3Fe_2(PO_4)_3$ at a magnetic field of $5 \times 10^{-2}$ T, are represented in Figure 2. The M versus $T$ curve shows a maximum at 28 K, with a very sharp profile, indicating the existence of an antiferromagnetic order in this compound. The high-temperature data ($T > 200$ K) are well-described by a Curie−Weiss law, with a Weiss temperature $\theta = -55$ K. The experimental effective moment per iron atom, at room temperature, is equal to 5.4 $\mu_B$. This value is slightly lower than the theoretical value of a free Fe(III) cation in a weak crystal field (5.92 $\mu_B$), which

(12) Christidis, P. C.; Rentzenperis, P. J. *Z. Kristallogr.* **1975**, *141*, 233.
(13) Chen, H. Y. *Mater. Res. Bull.* **1979**, *14*, 1583.
(14) Long, G. J.; Longworth, G.; Battle, P.; Cheetham, A. K.; Thundathil, R. V.; Beveridge, D. *Inorg. Chem.* **1979**, *18* (3), 624.
(15) Jirak, Z.; Salmon, R.; Fournès, L.; Menil, F.; Hagenmuller, P. *Inorg. Chem.* **1982**, *21*, 4218.
(16) Neel, L. *Ann. Phys.* **1948**, *12* (3), 137.
(17) Menil, F.; Pezat, M.; Tanguy, B. *C. R. Hebd. Seances Acad. Sci., Ser. C* **1975**, *281*, 849.

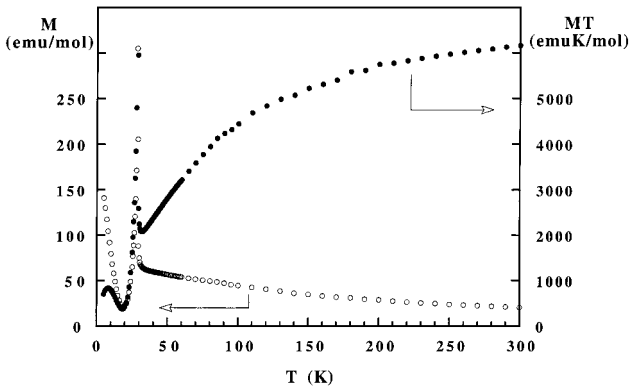


**Figure 2.** Thermal evolution of the molar magnetization $M$ and $MT$ for $\alpha$-$Li_3Fe_2(PO_4)_3$, at a magnetic field of 0.05 T.

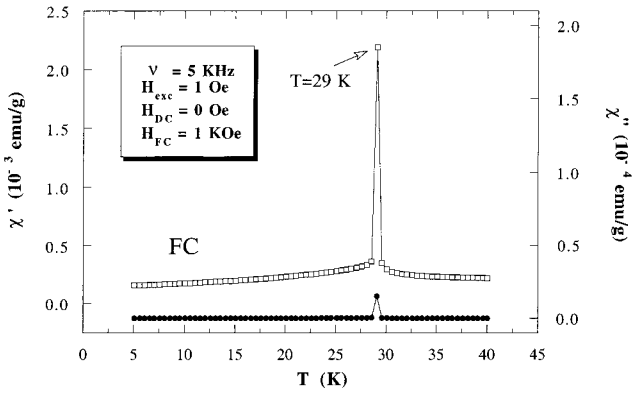


**Figure 3.** AC susceptibility measurements for $\alpha$-$Li_3Fe_2(PO_4)_3$, at 1 Oe and 5 kHz.

generally occurs for the most of antiferromagnetic compounds.

The $MT$ product reduces its value when the temperature decreases, confirming the predominance of antiferromagnetic interactions in this compound. However, the $MT$ curve exhibits a minimum at 31 K and then increases very rapidly to a maximum at 28 K. This behavior indicates the existence of an antiferromagnetic arrangement in the sample, with the appearance of a ferromagnetic component below the ordering temperature. The sharp peak in $-\mathrm{d}(MT)/\mathrm{d}T$ versus $T$ provides a $T_N = 28.0$ K. The AC susceptibility measurements (Figure 3) accurately show that the magnetic ordering transition occurs at 29 K. The ferromagnetic component that appears in the magnetic arrangement is revealed by the peak in the imaginary susceptibility $\chi''_m$ that accompanies the peak in $\chi'_m$ at 29 K.

The magnetization versus field curve registered at 25 K (Figure 4a) exhibits a hysteresis loop, becoming nearly linear up to 0.15 T. A weak magnetization of about 4.8 emu/mol is maintained at zero field, and the observed value for the coercitive field is about $-163 \times 10^{-4}$ T. Considering this result, field-cooled (FC) magnetization versus temperature measurements were carried out. The sample was field-cooled at 0.1 T, and zero-field-heated from several different temperatures below $T_N$ up to 40 K. The extraction of the maximum value of magnetization data from each curve and their representation versus temperature led to the curve given in Figure 4b. In that figure, one can observe a rapid increase of $M$ at 29 K, reaching a maximum value in the temperature range just below $T_N$. However, the

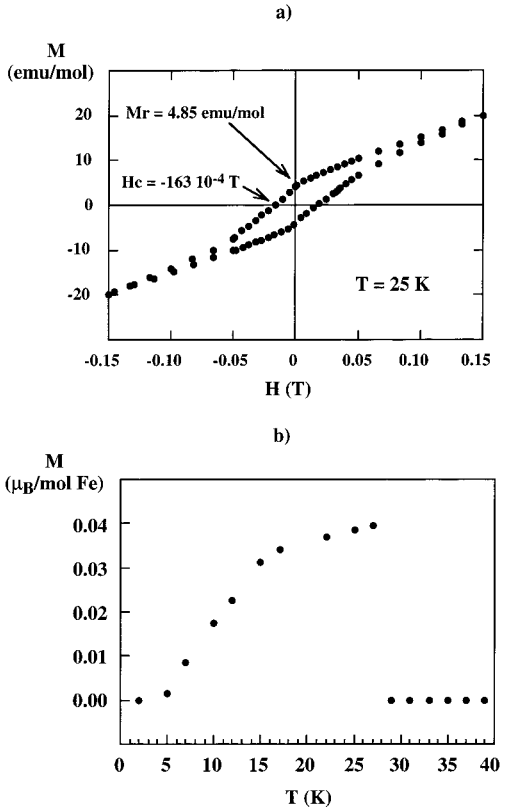


**Figure 4.** (a) Magnetization vs field curve registered at 25 K; (b) Temperature dependence of spontaneous magnetization.

remanent magnetization decreases again with decreasing temperature, approaching to zero when $T$ diminishes toward 0 K.

**Mössbauer Spectroscopy.** The $^{57}$Fe Mössbauer spectra of $\alpha$-$Li_3Fe_2(PO_4)_3$, recorded at several temperatures from 293 to 4.2 K, are shown in Figure 5. The spectrum in the paramagnetic state at 293 K is typical of high-spin Fe(III) ions in an octahedral environment. This spectrum was fitted to a doublet of Lorentzians of width $\Gamma = 0.25$ mm s$^{-1}$ with a quadrupole splitting $\Delta = 0.33$ mm s$^{-1}$. The isomer shift $\delta$ is 0.38 mm s$^{-1}$ relative to natural $\alpha$-Fe foil. These room temperature parameters are in good agreement with those reported for other related compounds[18,19] and confirm the existence of some distortions in the $FeO_6$ octahedra.

The experimental data from 28 to 4.2 K indicate that the material is magnetically ordered in that temperature range (Tables 1 and 2). In addition, it clearly appears, especially between 22.8 and 19 K, that the material exhibits more signals than the typical magnetic sextet that would result from the presence of a single uniform internal hyperfine field. In fact, these spectra are best understood in terms of two sextets, resulting from two different magnetic sublattices with essentially identical isomer and quadrupole shifts but slightly different internal hyperfine fields. The hyperfine parameters, line widths, and percentage areas of the two magnetic components obtained from the fits are given in Table 2. The temperature dependence of the two

(18) Beltrán-Porter, D.; Olazcuaga, R.; Fournès, L.; Menil, F.; Le Flem, G. *Rev. Phys. Appl.* **1980**, *15*, 1155.
(19) Salmon, R.; Olazcuaga, R.; Jirak, J.; Beltrán-Porter, D.; Fournès, L.; Menil, F.; Le Flem, G. *Solid State Chem., Proc. Eur. Conf., 2nd*. **1982**, *3*, 567 (Veldhoven, The Netherlands).

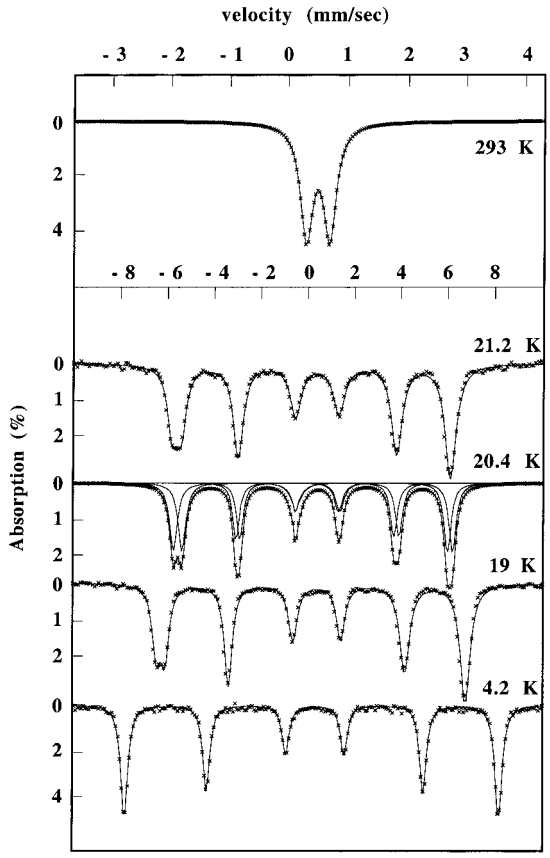


**Figure 5.** Mössbauer spectra of α-$Li_3Fe_2(PO_4)_3$ at different temperatures.

**Table 1. Mössbauer Parameters for the Spectra with a Unique Magnetic System**

| *T* (K) | *δ* (mm $s^{-1}$) | *B* (T) | Γ ($mms^{-1}$) |
|---|---|---|---|
| 4.2 | 0.546(6) | 54.9(4) | 0.43(1) |
| 8.0 | 0.552(8) | 53.0(5) | 0.42(1) |
| 10.0 | 0.550(6) | 52.7(4) | 0.43(1) |
| 12.0 | 0.548(6) | 51.2(4) | 0.43(1) |
| 14.0 | 0.535(8) | 49.7(5) | 0.42(1) |
| 16.0 | 0.530(10) | 47.3(5) | 0.42(1) |
| 17.3 | 0.531(8) | 46.6(5) | 0.42(1) |
| 23.5 | 0.52(1) | 32.0(8) | 0.42(1) |
| 25.0 | 0.52(1) | 28.9(8) | 0.43(1) |
| 26.0 | 0.50(1) | 25.2(8) | 0.44(1) |
| 27.0 | 0.51(1) | 19.9(9) | 0.45(1) |

**Table 2. Mössbauer Parameters for the Spectra with Two Magnetic Sublattices**

| *T* (K) | *δ* (mm $s^{-1}$) | *B* (T) | Γ (mm $s^{-1}$) | *A* (%) |
|---|---|---|---|---|
| | | Sublattice N. 1 | | |
| 19.0 | 0.53(1) | 43.2(5) | 0.42(1) | 49.2(4) |
| 20.4 | 0.53(1) | 40.7(5) | 0.41(1) | 49.8(4) |
| 21.2 | 0.52(1) | 39.0(5) | 0.40(1) | 49.4(4) |
| 22.8 | 0.53(1) | 35.4(5) | 0.40(1) | 49.7(4) |
| | | Sublattice N. 2 | | |
| 19.0 | 0.54(1) | 42.0(5) | 0.40(1) | 50.8(4) |
| 20.4 | 0.54(1) | 39.5(5) | 0.40(1) | 50.2(4) |
| 21.2 | 0.53(1) | 37.8(5) | 0.41(1) | 50.6(4) |
| 22.8 | 0.54(1) | 34.2(5) | 0.40(1) | 50.3(4) |

different hyperfine fields is reported in Figure 6. The difference between these two fields is shown in the inset of Figure 6. The maximum difference in the hyperfine field of the two different sublattices is 1.2 T. These two magnetic sublattices can be associated with the two crystallographically different iron sites in the structure.

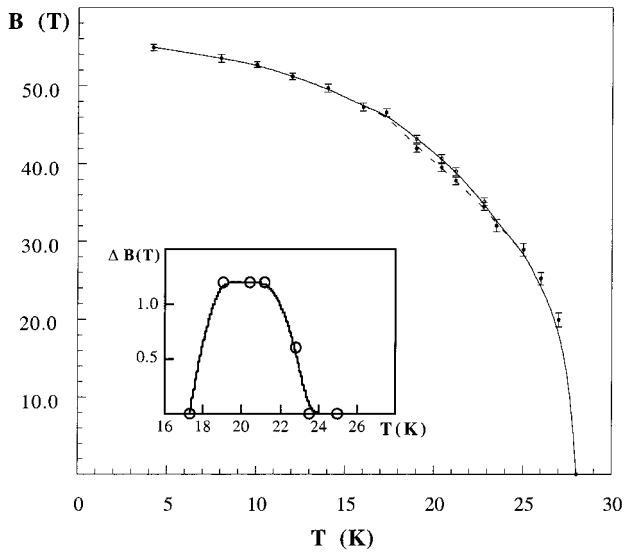


**Figure 6.** Temperature dependence of the hyperfine fields for the observed two Mössbauer sextets in the magnetically ordered α-$Li_3Fe_2(PO_4)_3$ phase. Inset: Difference between these fields as a function of temperature.

The Mössbauer data at 4.2 K can be attributed to a single magnetic spectrum of $\delta = 0.546(6)$ mm $s^{-1}$ and $B = 54.9(4)$ T. These parameters are consistent with those obtained for other iron(III) phosphate compounds.[20−23] At lowest temperatures, the hyperfine field is close to saturation at a value very near to the expected one of 55.0 T.[24]

## Discussion and Conclusions

The weak ferromagnetic component determined by magnetization measurements could be explained by either slight canting of the magnetic moments in the ordered state (weak ferromagnetism) or an incomplete compensation of the collinear arrangement of the moments (weak ferrimagnetism).[25] The canting phenomenon might originate a constant remanent magnetization below the ordering temperature, being in disagreement with the experimental results. Moreover, the hypothesis of canting cannot explain, in a satisfactory way, the existence of two different hyperfine fields for the iron ions in the Mössbauer spectra below $T_N$. The presence of weak ferrimagnetism is in good agreement with the existence of two octahedrically coordinated inequivalent sites, Fe(1) and Fe(2), in the structure of $Li_3Fe_2(PO_4)_3$.

The unit cell contains four Fe(III) ions of every independent site. Every Fe(III) ion of each sublattice establishes a complex scheme of exchange links with the nearest magnetic ions, via phosphate groups. The Fe−Fe interactions are intrinsically antiferromagnetic, but the resultant antiferromagnetic coupling between

(20) Korzenski, M. B.; Schimek, G. L.; Kolis, J. W.; Long, G. J. *J. Solid State Chem.* **1998**, *139*, 152.
(21) Long, G. J.; Gleitzer, C. *Hyperfine Interact.* **1990**, *62*, 147.
(22) Moya-Pizarro, T.; Salmon, R.; Fournès, L.; Le Flem, G.; Wanklyn, B.; Hagenmuller, P. *J. Solid State Chem.* **1984**, *53*, 387.
(23) Long, G. J.; Cheetham, A. K.; Battle, P. D. *Inorg. Chem.* **1983**, *22*, 3012.
(24) Johnson, C. E. *Hyperfine Interactions in Excited Nuclei*; Goldring, G., Kalish, R., Eds.; Gordon and Breach: New York, 1971.
(25) Carlin, R. L.; Van Duyneyeldt, A. J. *Magnetic Properties of Transition Metal Compounds*; Springer-Verlag: New York, 1977.

the crystallographically different Fe(1) and Fe(2) requires that each separate sublattice must be ferromagnetically coupled. The distances and angles for the Fe(1)−Fe(1) and Fe(2)−Fe(2) superexchange pathways do not have the same values. In this way, the Fe(1)−Fe(1) and Fe(2)−Fe(2) average distances are 5.02 and 5.26 Å, respectively, and the average superexchange angles at phosphorus are 110.6 and 112.2 ° (see Bykov et al.[10]). So, the value of the magnetic coupling constant, $J$, would not be the same for the two sublattices, implying two different $J_1$ and $J_2$ values in the Fe(1)−Fe(1) and Fe(2)−Fe(2) sublattices, respectively. This fact is confirmed by the presence of two different sextets with unidentical hyperfine fields in the Mössbauer spectra. The Fe(1)−Fe(2) antiferromagnetic interactions give rise to a global system with ferrimagnetic character. The saturation of the magnetic moments of both ferromagnetic sublattices to the total moment of the Fe(III) ions (about 5.4 $\mu_B$) would explain the disappearance of the remanent magnetic moment at the lower temperatures observed in this compound.

**Acknowledgment.** This work has been carried out with the financial support of the Ministerio de Educación y Ciencia (PB97-0640) and the UPV/EHU (UPV 169.310-EB149/98), which we gratefully acknowledge.

CM991069C